International Food Research Journal 32(3): 744 - 761 (June 2025)

Journal homepage: http://www.ifrj.upm.edu.my



Formulation and characterisation of fruit- and vegetable-based gel/paste for potential application in food 3D printing

¹Sabri, N. S., ²Mohd Shah, M. I. H. and ¹*Yusvana, R.

¹Department of Chemical Engineering Technology, Faculty of Engineering Technology (B-SMAT Focus Group), Universiti Tun Hussein Onn Malaysia, Pagoh, Higher Education Hub, 84600 Pagoh, Johor, Malaysia ²Faculty of Applied Sciences and Technology, Universiti Tun Hussein Onn Malaysia, Pagoh, Higher Education Hub, 84600 Pagoh, Johor, Malaysia

Article history

Received: 17 July 2024 Received in revised form: 4 May 2025 Accepted: 22 May 2025

Keywords

food 3D printing, fruit-based gel, hydrocolloids, personalised nutrition, antioxidant activity

Abstract

One of the major barriers to developing food three-dimensional (3D) printing for personalised nutrition applications is the lack of food materials that can maintain structural integrity, nutritional adaptability, and sustainability. The present work addressed these challenges by creating and evaluating the gel paste from selected fruit and vegetable ingredients for food 3D printing applications. The main ingredients included high-fat avocado, fermented black garlic, lemon juice, celery, potato starch (PS), and xanthan gum (XG), which were used as thickeners. Optimal paste formulations offered robustness for 3D shape and form while maintaining desired nutritional content. The present work then developed four different paste types, containing different hydrocolloid compositions for 3D printing via a 0.5 mm syringe for quick extrusion testing. Analysis involved physicochemical parameters such as water content (WC), texture, antioxidant activity, carbohydrates, and vitamin C. Results indicated that moisture content played a crucial role in the structural stability of the paste, with the type 3 formulation (5% PS and 2% XG) demonstrating optimal moisture balance and structural integrity. Texture analysis indicated that type I pastes, which were composed of 3% PS and 1% XG, exhibited optimal hardness (7.427 N) and adhesiveness (-5.341 N), alongside adequate WC (83.37%) for effective extrusion and 3D shaping. Nutritional analysis indicated that the avocado-rich paste (type IV) had the highest antioxidant concentration, whereas the black garlic-rich paste (type I) exhibited the highest sugar content. The paste rich in lemon juice (type II) offered the highest vitamin C concentration, an important enhancement to nutritional value. The present work demonstrated the possibility of designing nutrient profiles for food 3D printing that enable novel culinary use and personalised nutrition. The findings would contribute to the field of food technology, with an emphasis on personalised nutrition.

DOI

https://doi.org/10.47836/ifrj.32.3.10

© All Rights Reserved

Introduction

The rapid evolution of technology in recent years has resulted in transformative shifts across nearly all domains of human activities. Among these advancements, three-dimensional (3D) food printing is an important culinary technology innovation, likely redefining food production and consumption paradigms. This technology enables the fabrication of intricate, customisable food structures with diverse geometries, ingredient compositions, and nutritional profiles, offering unprecedented versatility in gastronomic design (Pulatsu and Lin, 2021).

The 3D printing, or additive manufacturing, originated several decades ago as a tool for industrial prototyping, with early applications concentrated in the aerospace and automotive sectors. However, its adaptation to the food industry represents a more recent development. Initial breakthroughs occurred in 2007, when researchers at Cornell University engineered the first functional food 3D printer (Periard *et al.*, 2007). While early iterations focused on rudimentary chocolate-based constructs, subsequent advancements have expanded capabilities to include complex items such as textured pasta, multi-ingredient meals, and nutritionally optimised

*Corresponding author. Email: rama@uthm.edu.my dishes—a stark departure from the technology's nascent form.

As accessibility to 3D printing systems increased during the mid-2000s, commercial and scientific entities began exploring novel applications. A critical driver of innovation arose from space exploration initiatives, particularly National Aeronautics and Space Administration (NASA) 2013 experiments with 3D-printed foods to enhance dietary variety for astronauts during prolonged missions This research built upon (SavorEat, 2023). foundational work from 2006, when Cornell's engineering team pioneered open-source, multimaterial 3D printing frameworks that later informed edible material deposition techniques.

The operational principles of food-grade 3D printing mirror conventional additive manufacturing, with key distinctions. Rather thermoplastics or metals, food printers employ extrusion-based deposition of edible pastes, such as doughs, pureed vegetables, or protein-rich blends to construct layer-by-layer geometries (Pulatsu and Lin, 2021). These viscoelastic "inks" require precise rheological control to maintain structural fidelity specialised printing, necessitating during formulations that balance extrudability with postprocessing stability. Such innovations circumvent the need for synthetic polymers, instead of utilising nutrient-dense edible matrices to achieve functional food architectures.

Food 3D printing enables precise control over the final product's geometry, nutritional composition, and sensory attributes, akin to the modular adaptability of LegoTM systems in assembling diverse structures. Upon uploading a Computer-Aided Design (CAD) file to the printer, the device concurrently initiates thermal processing of the raw material. This heating phase enhances the material's plasticity, eliminating the need for boiling and ensuring optimal extrudability. Guided by the digital template, the printer's nozzle deposits the thermally modified edible material in successive layers, forming a three-dimensional product. The process is further stabilised by incorporating gelling agents, which ensure structural integrity during deposition (Tomašević et al., 2021).

Consequently, this new technology breaks traditional thoughts on preparing or consuming food. Its applications range from personalised nutrition solutions to making a broader application of culinary innovation to therapeutic dietary treatments for

diseases. These applications have great societal and industrial significance (Varvara *et al.*, 2021). With the gradual technological barrier overcome, food 3D printing is expected to change contemporary gastronomy by combining convenience, customisation, and cutting-edge food art.

Despite these developments, significant knowledge gaps remain in the rheological and functional behaviour of the 'inks' for edible printing. The present work described the development of a fruit-based gel, from avocado, for 3D food printing and its characterisation. By tailoring the composition of the paste to satisfy certain nutritional and printability requirements, the present work aimed towards addressing one of the main challenges in the area: the lack of health-oriented, custom edible 'inks'. The present work also aimed to establish foundational guidelines for developing sustainable, nutritionally adaptable 3D-printed foods based on the empirical study of the material properties through the extrusion process. These efforts align with broader objectives to advance culinary innovation and promote resourceefficient food production systems.

Materials and methods

Processing of main ingredients

The primary components were high-fat avocado, black garlic, lemon juice, and celery. Avocado was chosen for its lipid-dense content, which improves smoothness and structural integrity during extrusion. Black garlic, a fermented product, provides natural sugars (for carbohydrate content) and antioxidants, supporting the objective of nutritional customisation. Lemon juice enhances flavour with its acidity, acts as a natural preservative, and provides vitamin C. Celery contributes dietary fibre and vegetal nuances, enhancing the paste's consistency. Potato starch (PS) and xanthan gum (XG) were selected as hydrocolloids for their synergistic thickening attributes: PS imparts viscosity and water retention, whereas XG facilitates shearthinning behaviour essential for 3D printing extrusion. As specified in the study's objectives, these elements collectively enhanced printability, nutrient diversity, and structural integrity.

All ingredients were procured from local supermarkets and stored in the refrigerator at 4°C for a maximum of 2 d before use (Pant *et al.*, 2020). The ingredients were diced, washed, and peeled as needed before being blended for 5 to 10 min to obtain a

puree-like consistency (base paste). In order to avoid clogging the syringe nozzle (0.5 mm diameter) used in 3D printing, the puree was sieved through a mesh 0.2 mm in size to ensure particle uniformity.

Different hydrocolloid compositions

Hydrocolloid-based formulations were systematically evaluated to identify optimal combinations for 3D food printing applications.

Blends of PS (3 - 10% (w/w)) and XG (1 - 2% (w/w)) were prepared to investigate their influence on the avocado-derived pastes' structural and rheological properties. Four distinct formulations were tested: (i) 3% PS + 1% XG; (ii) 3% PS + 2% XG; (iii) 5% PS + 2% XG; and (iv) 10% PS + 1% XG (Table 1). Each mixture was standardised to a total mass of 80 g, comprising a base paste augmented with varying PS:XG ratios, as detailed in Table 1.

Table 1. Samples' composition: (a) different compositions of potato starch and xanthan gum, and (b) different ratio contents of each sample.

Ingredient	Type 1	Type 2	Type 3	Type 4
Potato starch, PS (g)	2.4	2.4	4.0	8.0
Xanthan gum, XG (g)	0.8	1.6	1.6	0.8
Base paste (g)	76.8	76.0	74.4	71.2

Ingredient	Base paste	I	II	III	IV
Black garlic	0.080	0.148	0.070	0.067	0.051
Lemon juice	0.140	0.130	0.245	0.118	0.088
Celery	0.190	0.176	0.167	0.319	0.119
Avocado	0.590	0.546	0.518	0.496	0.742

Type 1: 3% (w/w) PS with 1% (w/w) XG; Type 2: 3% (w/w) PS with 2% (w/w) XG; Type 3: 5% (w/w) PS with 2% (w/w) XG; and Type 4: 10% (w/w) PS with 1% (w/w) XG). I: rich in black garlic; II: rich in lemon juice; III: rich in celery; and IV: rich in avocado.

To evaluate printability, the pastes were required to exhibit sufficient viscoelasticity for layer-by-layer deposition while retaining structural fidelity post-extrusion. The PS:XG ratio was hypothesised to govern textural attributes such as viscosity, shear-thinning behaviour, and yield stress parameters directly impacting extrudability and shape retention (Zhao *et al.*, 2024). These properties were analysed to determine their alignment with the functional demands of food 3D printing, including compatibility with nozzle geometries and printing speeds.

The compositional variations were designed to elucidate the interplay between PS (a primary thickener) and XG (a rheology modifier). As demonstrated in prior studies, synergistic interactions these hydrocolloids between can enhance pseudoplasticity, a prerequisite for precise extrusion in additive manufacturing (Zhao et al., 2024). By correlating formulation data with performance metrics, the present work established a framework for tailoring edible inks to specific nutritional or industrial requirements, thereby expanding their potential applications.

Syringe checks for suitable 'ink' materials for food 3D printing applications

A syringe-based screening method was employed to rapidly assess the suitability of edible ink formulations for 3D food printing applications. A 0.5-mm injection syringe was utilised to extrude preliminary 3D structures, enabling the identification of formulations capable of retaining structural integrity at room temperature while solidifying into geometrically stable forms with acceptable viscoelastic properties. This approach prioritises two critical criteria: (i) the ink's ability to maintain shape fidelity post-extrusion, and (ii) its capacity to transition into a cohesive 3D structure with textural characteristics suitable for consumption.

During this early stage of development, syringe-based extrusion over direct testing with commercial 3D printers is beneficial. This method reduces the resources used by conserving material, minimising waste, accelerating the iterative process, and the optimisation of 'ink' compositions is far less complicated. In addition, the accuracy of syringes enables careful investigation of extrusion

characteristics such as paste property, shear-thinning behaviour, flow uniformity, and the printing process itself. They give quick information about the ink compatibility with the nozzle geometry and the layerby-layer deposition. Syringe screening maximises the potential for scaling up a suitable ink for industrial or culinary use by reducing formulation changes and development time.

Sample compositions

Four distinct paste formulations were prepared to investigate their compositional and functional variability, each incorporating a unique primary ingredient—black garlic, lemon juice, celery, or avocado. The study focused on quantifying carbohydrate content, vitamin C levels, and antioxidant activity across these formulations, with detailed compositional ratios provided in Table 1. Each sample was standardised to a total mass of 80 g, ensuring consistency in comparative analyses while enabling variations in taste profiles and nutritional characteristics.

Furthermore, fermented black garlic contributed to pronounced umami depth and aromatic complexity (Bedrníček et al., 2021), whereas celery introduced herbaceous freshness. Lemon juice provided citrus acidity to balance richer flavours, while avocado enhanced textural uniformity through its natural emulsification capacity, yielding a smooth, These ingredient-specific cohesive matrix. functionalities diversified sensory attributes and expanded potential health applications, aligning with personalised nutrition and culinary adaptability demands. The systematic variation in component ratios across samples facilitated an evaluation of how ingredient interactions influence physicochemical properties and consumer-oriented qualities.

Physicochemical properties of pastes

The physicochemical properties of the gel pastes—including texture, moisture content, antioxidant activity, and visual morphology—were systematically analysed to evaluate their suitability for 3D food printing. These characteristics were assessed using standardised experimental protocols to establish correlations between compositional variables and functional performance.

Water content analysis of pastes

Water content (WC), a critical parameter influencing printability and post-extrusion structural

stability, was quantified via thermogravimetric analysis. Approximately 5 g of each paste variant was uniformly spread on aluminium foil and dried in a hot-air oven at 150°C until reaching constant mass. Pre- and post-drying weights were recorded to calculate WC using Eq. 1, with results compared across the four formulations (types 1 - 4). Hydrocolloid incorporation, as outlined by Pant et al. (2020), was designed to modulate water-binding capacity, thereby optimising gel consistency for shape retention during layer-by-layer deposition. This methodological approach enabled the identification of formulations balancing adequate plasticity for extrusion with sufficient rigidity for dimensional fidelity, addressing a key requirement for scalable 3D food printing applications.

WC (%) =

 $\frac{\text{weight sample before drying-weight sample after drying}}{\text{weight sample before drying}} \times 100$

(Eq. 1)

Texture analysis of pastes

Texture analysis was conducted to assess the mechanical properties of the paste, specifically hardness and adhesiveness, which are critical determinants of printability in 3D food applications. A texture analyser (Razavi and Karazhiyan, 2012) equipped with a 40° conical Perspex probe was employed under standardised testing parameters: pretest speed of 2.00 mm/s, post-test speed of 10.00 mm/s, and a penetration depth of 2 mm. All four formulations (types 1 - 4) were subjected to this protocol to evaluate their capacity to maintain structural integrity during extrusion and subsequent layer adhesion. Hardness measurements quantified the resistance of the paste to deformation under compressive force, while adhesiveness reflected its tendency to adhere to the printing nozzle or substrate. These parameters collectively informed the selection of formulations optimised for precise deposition and shape retention, aligning with the functional demands of 3D food printing systems.

Nutritional analysis of pastes

Nutritional profiling of the paste formulations focused on three key parameters: antioxidant activity, carbohydrate content (primarily glucose), and vitamin C concentration. These metrics were selected to align with the study's emphasis on personalised nutrition, wherein ingredient modifications (e.g.,

avocado and black garlic) were engineered to tailor formulations to specific dietary requirements. Antioxidant capacity was quantified to assess the potential for mitigating oxidative stress, positioning the pastes as functional food candidates for health-focused consumers. Carbohydrate analysis targeted energy-providing components, with implications for dietary regimens such as diabetic or low-carbohydrate meal plans. Concurrently, vitamin C levels were measured due to their critical role in immune function and overall physiological well-being.

Antioxidant activity of pastes

The antioxidant activity of the gel pastes was evaluated using the DPPH (2,2-diphenyl-1picrylhydrazyl) radical scavenging assav. methanolic DPPH solution (0.1 mM) was prepared by dissolving 4 mg of DPPH in 100 mL of methanol. To account for the compound's photosensitivity, the solution was stored in a 250-mL amber conical flask or aluminium foil-covered tubes, as recommended by Xiao et al. (2020), and incubated in darkness for 2 h to stabilise. For the assay, 1 mL of the DPPH solution was mixed with 1 mL of the extract sample at varying concentrations in a test tube wrapped with aluminium foil. After 30 min of incubation in the dark at room temperature, the absorbance was measured at 517 nm a UV-Vis spectrophotometer. scavenging activity was calculated using Eq. 2:

Scavenging activity =

$$\left(\frac{A_{control} - A_{sample}}{A_{control}}\right) x 100$$
 (Eq. 2)

where, $A_{control}$ = absorbance of the DPPH solution without the sample, and A_{sample} = absorbance of the DPPH solution of the test sample. A calibration curve was constructed using ascorbic acid to standardise the analysis. A stock solution of ascorbic acid (10 mg in 10 mL methanol) was serially diluted to concentrations ranging from 0.02 to 0.1 mg/mL. These standards, prepared in foil-covered tubes, were mixed with DPPH solution, incubated for 30 min in darkness, and their absorbances measured at 517 nm to generate the standard curve.

Approximately 10 mg of each test sample (base paste and types I - IV) was dissolved in 10 mL of methanol for sample analysis. Next, 1 mL aliquot of each sample solution was combined with 1 mL of DPPH solution and 3 mL of methanol in an

aluminium foil-covered test tube. The mixture was vortexed, incubated in the dark for 30 min, and centrifuged to clarify the suspension. The absorbance of the resulting solution was measured at 517 nm and compared against the ascorbic acid standard curve to activity. quantify the antioxidant Control measurements (DPPH solution without samples) and triplicate analyses ensured reproducibility. This method enabled the assessment of free radical scavenging capacity, with lower absorbance values indicating higher antioxidant potential due to DPPH radical neutralisation by the test samples. The use of light-protected containers and timed incubation steps minimised photodegradation artifacts, ensuring reliable results (Flieger and Flieger, 2020; Xiao et al., 2020).

Carbohydrate analysis of pastes

The total carbohydrate content of the gel paste samples was quantified using the 3,5-dinitrosalicylic acid (DNS) assay, as described by Božinović et al. (2023). In this method, carbohydrates react with DNS under high-temperature alkaline conditions to produce a red-brown colour, proportional to reducing sugar concentration. For analysis, 1 mL of each sample was combined with 1 mL of DNS reagent in a test tube, boiled in a water bath at 90°C for 5 min, and cooled to room temperature. The mixture was diluted with up to 10 mL of distilled water to stabilise the colour, and absorbance was measured at 540 nm using a UV-Vis spectrophotometer. Glucose served as the reference standard, with a stock solution (0.1 g/mL) serially diluted to generate a calibration curve spanning concentrations of 0 - 1 g/mL. Each standard solution (1 mL) was mixed with 2 mL of DNS reagent, heated at 90°C for 5 min, cooled, and diluted with 7 mL of distilled water before absorbance measurement. The resulting data were plotted to establish a linear relationship between glucose concentration and absorbance, enabling quantification of carbohydrate content in samples.

For sample preparation, 1 g of each gel paste variant (base paste, I, II, III, and IV) was dissolved in 10 mL of distilled water. Next, 1 mL aliquot of the dissolved sample was mixed with 2 mL of DNS reagent, heated in a water bath at 90°C for 5 min, and cooled. The reaction mixture was diluted with 7 mL of distilled water, and absorbance was recorded at 540 nm. The glucose-equivalent carbohydrate concentration in each sample was calculated using the

standard curve equation derived from the linear regression of absorbance versus glucose concentration. This method ensured precise quantification of reducing sugars, with the DNS assay's specificity for free carbonyl groups in carbohydrates minimising interference from nonreducing sugars. All steps, including heating and dilution, were rigorously controlled to maintain consistency and accuracy, as outlined in the referenced protocol (Božinović et al., 2023).

Vitamin C analysis of pastes

The gel paste samples' vitamin C (ascorbic acid) content was determined using a redox titration method based on the stoichiometric reaction between ascorbic acid and iodine, adapted from Helmenstine (2007). An iodine titrant solution (0.005 M) was prepared by dissolving 2 g of potassium iodide (KI) and 1.3 g of iodine (I₂) in a minimal volume of distilled water, followed by vigorous stirring until complete dissolution. The solution was transferred to a 1-L volumetric flask, and the volume was adjusted to the mark with distilled water. Next, 0.5% starch indicator solution was prepared to enhance endpoint detection by dissolving 0.25 g of soluble starch in 50 mL of near-boiling water within a 100-mL conical flask. The mixture was stirred until a translucent suspension formed, cooled to room temperature, and stored at 4°C until use. For the assay, 10 mL of sample extract was combined with 10 mL of 1% starch solution. The mixture was titrated with standardised iodine solution (0.01 N) until a stable blue-black colour persisted for 20 sec, marking the endpoint. The method was validated using known ascorbic acid concentrations to ensure accuracy and reproducibility, with triplicate measurements performed for all samples and standards.

A standard curve was generated using pure ascorbic acid to quantify vitamin C in test samples. A stock solution (1 mg/mL) was prepared by dissolving 0.25 g of ascorbic acid in 100 mL of distilled water, then diluting to 250 mL. For titration, 25 mL of the stock solution was transferred to a 125-mL Erlenmeyer flask, and 1 mL of starch indicator was added. The burette was rinsed and filled with iodine titrant, and the initial volume was recorded. Titration proceeded until the first persistent blue colour appeared after 20 sec of swirling, with the final volume recorded. This process was repeated three times to establish precision. The average iodine consumption was used to calculate the ascorbic acid

concentration based on the 1:1 molar ratio between vitamin C and iodine ($C_6H_8O_6 + I_2 \rightarrow C_6H_6O_6 + 2I^- + 2H^+$). The standardised method demonstrated linearity across the tested range, with rigorous control of reaction conditions to minimise oxidation artifacts.

For sample analysis, 50 g of each gel paste variant (base paste, I - IV) was homogenised in 25 mL of distilled water, filtered to remove particulates, and adjusted to 100 mL with distilled water. Next, 25 mL aliquot of the filtrate was pipetted into a titration flask, diluted with 150 mL of distilled water, and mixed with 1 mL of starch indicator. The solution was titrated with iodine titrant under conditions identical to the standard, and the sustained blue-black coloration determined the endpoint. Triplicate titrations were performed for each sample, and the average volume of iodine consumed was substituted into the stoichiometric equation (Eqs. 3 and 4) to calculate vitamin C concentration:

$$\frac{volume\ of\ l\ used\ for\ standard\ (ml)}{mass\ of\ ascorbic\ acid\ (0.25\ g)} = \frac{volume\ of\ l\ used\ for\ sample\ (ml)}{mass\ of\ sample\ (x\ g)} \tag{Eq. 3}$$

$$vitamin C = \frac{mass \ of \ sample(x \ g)}{volume \ of \ sample(25 \ ml)}$$
 (Eq. 4)

Results and discussion

This section outlines the findings from the experiments conducted in detail in the methodology section. Moisture content and texture analysis were performed to investigate the physicochemical properties of the 3D paste with various hydrocolloid formations (types 1, 2, 3, and 4). Analyses of antioxidants, carbohydrates, and vitamin C were performed to examine the nutritional profile of the 3D pastes (base paste, types I, II, III, and IV).

Water content analysis of pastes

The structural integrity and printability of 3D food pastes are critically influenced by moisture content, as underscored by prior studies (Bhat *et al.*, 2021; Hussain *et al.*, 2022). In the present work, incorporating hydrocolloids-PS and XG-modulated the water retention of the formulations. The base paste, devoid of hydrocolloids, exhibited the highest moisture content (88.57%), indicating its unmodified water-binding capacity. However, incremental additions of PS and XG across the formulations (types 1 - 4) led to a progressive reduction in

moisture, as illustrated in Figure 1. This trend aligns with the hygroscopic nature of hydrocolloids, which competitively bind free water through their polysaccharide matrices, thus lowering overall water availability (Hussain *et al.*, 2022). The observed

moisture reduction underscored the pivotal role of hydrocolloid concentration in tailoring the rheological properties essential for extrusion-based 3D printing.

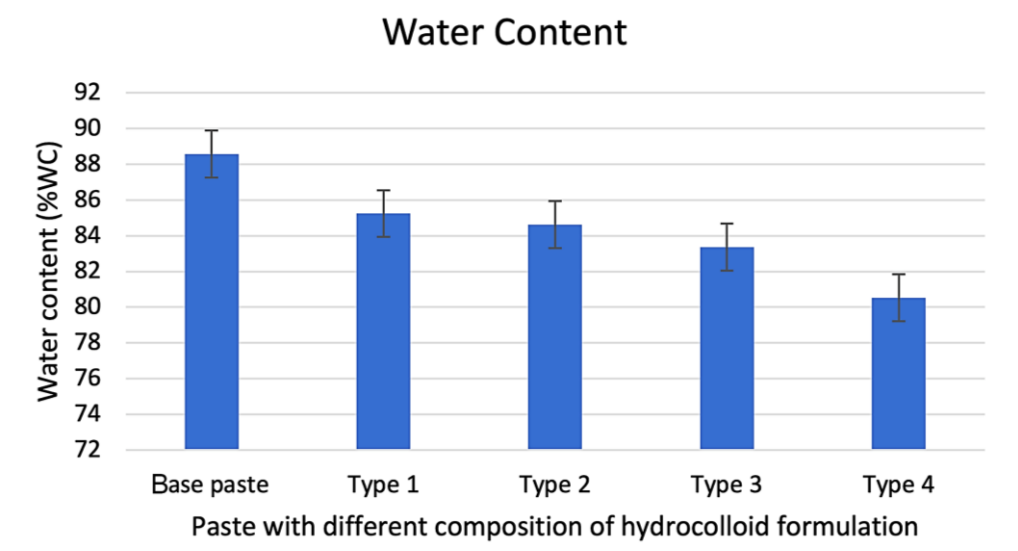


Figure 1. Water contents of different compositions of hydrocolloid formulations when drying in oven at 150°C for approximately 2 h. Data were collected three times. Type 1: 3% (w/w) PS with 1% (w/w) XG; Type 2: 3% (w/w) PS with 2% (w/w) XG; Type 3: 5% (w/w) PS with 2% (w/w) XG; and Type 4: 10% (w/w) PS with 1% (w/w) XG.

Among the tested formulations, type 3 [5% (w/w) PS and 2% (w/w) XG] demonstrated the lowest moisture content (83.37%), a characteristic that conferred optimal structural stability during printing. This formulation achieved a delicate equilibrium between dryness and plasticity, minimising postextrusion deformation while ensuring smooth material flow through the nozzle. In contrast, type 1 [3% (w/w) PS and 1% (w/w) XG] and type 2 [3% (w/w) PS and 2% (w/w) XG] exhibited higher moisture levels (85.24% and intermediate values, respectively), which, while suitable for extrusion, posed challenges in maintaining intricate geometries post-deposition. Notably, type 4 [10% (w/w) PS and 1% (w/w) XG] deviated from this balance, with excessive dryness (moisture content below type 3) leading to brittleness and nozzle clogging, compromising print fidelity. These findings corroborated previous assertions that hydrocolloid interactions with water governed the paste's ability to retain shape without sacrificing extrudability (Ji et al., 2022).

The interplay between moisture content and printability was further elucidated by the performance of type 3, which exhibited an optimal viscosity-solidification balance. Gu *et al.* (2020) noted that

reduced WC mitigated undesirable fluidity during extrusion, ensuring dimensional accuracy in the printed structure. The base paste's high moisture (88.57%) resulted in excessive flow, leading to structural collapse, whereas type 3's intermediate moisture facilitated controlled deposition and rapid stabilisation post-extrusion. This behaviour aligned with shear-thinning requirements for 3D food inks, where viscosity must decrease under shear stress for extrusion but recover swiftly to retain shape (Hussain et al., 2022). Consequently, type 3's formulation highlighted the importance of hydrocolloid ratios in modulating WC, and established a benchmark for developing nutritionally customisable inks with robust printability.

The present work examined moisture content under controlled room-temperature conditions. However, environmental factors like temperature and humidity may additionally affect stability and printability. Increased temperatures can enhance moisture loss, which may jeopardise structural integrity, as evidenced by the drier consistency observed in type 4. High humidity may enhance water absorption, thereby affecting paste viscosity. These factors underscore the necessity of controlled environments in 3D printing to sustain optimal

moisture levels. Future research should systematically assess the impacts of temperature and humidity on extrusion and shape retention, reinforcing our findings that moisture content is critical for printability (Gu *et al.*, 2020). The existing formulations exhibited robustness under standard ambient conditions, as demonstrated by successful 3D shaping (Figure 2).

Texture analysis of pastes

The textural properties of 3D food printing pastes, particularly hardness and adhesiveness, are

critical determinants of printability and structural fidelity, as these parameters govern deformation resistance and interlayer cohesion during extrusion (Zhu *et al.*, 2019). As illustrated in Figure 2, the hardness values of the tested formulations (types 1 - 4) exhibited nuanced variations, with type 1 (7.427 N) and type 3 (7.427 N) demonstrating superior resistance to deformation compared to types 2 and 4 (7.303 N). This marginal disparity in hardness reflected the differential capacity of hydrocolloid-stabilised matrices to withstand mechanical stress during deposition. Notably, type 1's optimal

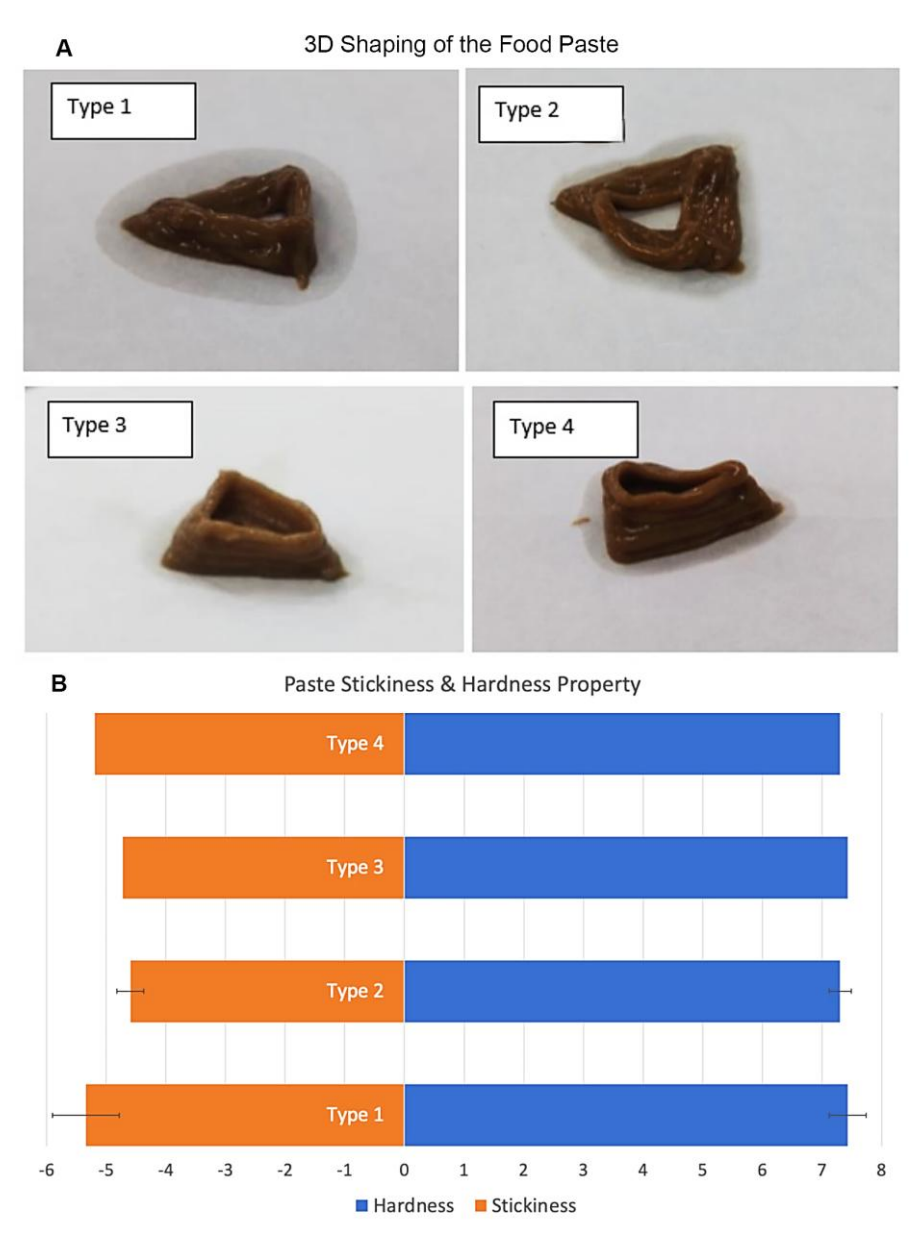


Figure 2. (A) 3D shaping of 3D food printing paste using a 0.5 mm syringe at room temperature. Type 3 is the optimum formulation. **(B)** Texture analysis of different compositions of paste formulation based on hardness and adhesiveness (stickiness). Pre-test speed at 2.00 mm/sec; post-test speed at 10.00 mm/sec; distance at 2 mm; and probe of 40° cone Perspex. Data were collected three times. Type 1: 3% (w/w) PS with 1% (w/w) XG; Type 2: 3% (w/w) PS with 2% (w/w) XG; Type 3: 5% (w/w) PS with 2% (w/w) XG; and Type 4: 10% (w/w) PS with 1% (w/w) XG.

hardness aligned with the requirements for precise layer stacking in 3D printing, as excessive rigidity can impede extrusion, while insufficient firmness risks collapse (Derossi al., structural et Adhesiveness, a measure of internal bonding strength (Zhao et al., 2024), further distinguished the formulations: type 1 exhibited the adhesiveness (-5.341 N), indicative of reduced stickiness, whereas type 2 (-4.595 N) and type 3 (-4.720 N) demonstrated higher cohesive forces, potentially complicating nozzle release. These findings underscored the necessity of balancing hardness and adhesiveness to achieve dimensional accuracy and extrusion efficiency.

The interplay between ingredient composition and hydrocolloid functionality emerged as a key factor influencing textural outcomes. For instance, the elevated fat content in the avocado-enriched type IV paste likely enhanced cohesiveness through hydrophobic interactions with PS and moderating hardness (7.303 N) while preserving structural stability (Figure 2). Conversely, the acidic environment imparted by lemon juice in type II may have inhibited starch gelatinisation, resulting in reduced hardness (7.303 N) compared to types I and III. The shear-thinning behaviour of XG, as noted in prior studies, contributed to decreased instability during extrusion, enhancing printability across formulations (Wang et al., 2024). Furthermore, the fibrous matrix from celery in type III improved water retention (83.37% moisture), fostering a balance between rigidity and plasticity. These observations highlighted the critical role of ingredienthydrocolloid synergies in modulating rheological behaviour, where compositional variations would directly impact textural attributes essential for 3D printing.

Type 1 emerged as the optimal formulation for 3D food printing applications, combining moderate hardness with minimised adhesiveness to ensure precise deposition and shape retention. The reduced stickiness (-5.341 N) in type 1, attributed to the complex carbohydrates in black garlic, likely facilitated hydrogen bonding with PS and XG, thus stabilising the paste matrix without excessive cohesion. This formulation's textural profile aligned with the prerequisites for extrusion-based printing, where controlled flow and rapid structural recovery post-deposition are paramount (Derossi *et al.*, 2020).

In contrast, type 4's higher PS content (10% (w/w)) introduced excessive dryness, hence compromising extrudability and layer adhesion. The results collectively emphasised that ingredient-specific interactions—such as lipid-starch retardation, acidinduced gelatinisation inhibition, and fibre-enhanced water retention—must be carefully optimised to tailor paste formulations for functional 3D printing. This systematic evaluation of texture-structure relationships would advance the rational design of hydrocolloid-based inks, enabling customisation for diverse nutritional and mechanical requirements in additive food manufacturing.

The interaction between hydrocolloids and ingredients affected texture and stability. For example, the high fat content of avocado (type IV) likely interacted with PS and XG, enhancing cohesiveness, as evidenced by its moderate hardness (7.303 N) and structural stability (Figure 2). Lipids retrogradation, decrease starch thereby preserving smooth extrusion. Lemon juice's acidity (type II) may partially inhibit starch gelatinisation, resulting in a lower hardness of 7.303 N compared to types I and III. Furthermore, XG's shear-thinning properties reduced instability, thereby enhancing printability. Celery's fibre (type III) may have interacted with hydrocolloids to enhance water retention (83.37% moisture), thereby balancing rigidity and plasticity. Black garlic's sugars (type I) enhanced paste adhesiveness (-5.341 N), likely attributed to starch-sugar interactions influencing hydrogen bonding. These interactions underscored significance ingredient-hydrocolloid of compatibility in optimising texture and stability for 3D printing.

Nutritional analysis of pastes

This section examines the nutrient composition of formulated paste with varying ingredient richness. The result of the analysis is summarised and displayed in Figure 3. The base paste consisted of common ingredients, whereas pastes I, II, III, and IV were characterised by their richness in black garlic, lemon juice, celery, and avocado. The present work aimed to analyse the nutrient content in pastes when specific ingredient modifications occurred, to assess its applicability for personalised nutrition in food 3D printing.

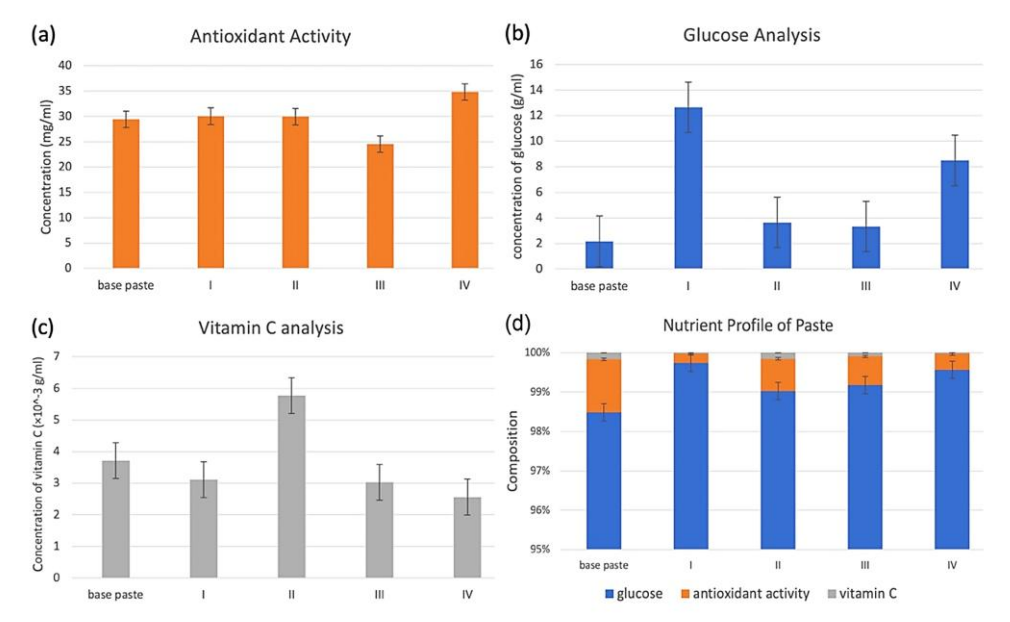


Figure 3. Nutritional profile of paste samples. **(a)** Antioxidant activity of formulated paste; **(b)** carbohydrate analysis of formulated paste; **(c)** vitamin C analysis of formulated paste, the standard solution obtains 86.43 mL of iodine solution to reach the endpoint; and **(d)** nutritional profile of formulated paste. Data were collected three times. I: rich in black garlic; II: rich in lemon juice; III: rich in celery; and IV: rich in avocado.

Antioxidant activity of pastes

The antioxidant potential of food formulations is an indicator of their nutritional value and healthpromoting properties, offering insights into their capacity to mitigate oxidative stress (Vlaicu et al., 2023). In the present work, the antioxidant activities of four paste formulations—enriched with black garlic (type I), lemon juice (type II), celery (type III), and avocado (type IV)—were quantitatively assessed using UV-Vis spectrophotometry, with DPPH radical scavenging assays conducted at 517 nm (Figure 3a). The results revealed marked disparities in antioxidant concentrations, ranging from 24.55 mg/mL in celeryrich type III to 34.84 mg/mL in avocado-rich type IV. These variations underscored the intrinsic differences bioactive compound profiles among the ingredients, highlighting their distinct roles in enhancing the antioxidant capacity of the formulated pastes.

Black garlic (type I) exhibited a moderate antioxidant concentration of 30.04 mg/mL, attributable to its rich phenolic and flavonoid contents, which are well-documented for their radical-scavenging properties (Qiu *et al.*, 2020; Choudhary *et al.*, 2022). Despite its fermentation process, which enhances bioactive compound availability, black garlic's antioxidant level was slightly surpassed by lemon juice (type II, 29.95

mg/mL). Citrus fruits, including lemons, are renowned for their high vitamin C and flavonoid concentrations, synergistically contributing to antioxidant efficacy (Alfadul and Hassan, 2016). The proximity in antioxidant values between types I and II suggested that both ingredients offered comparable, though chemically distinct, mechanisms for oxidative stress mitigation.

Celery-enriched type III demonstrated the lowest antioxidant activity (24.55 mg/mL), yet its contribution remained noteworthy. Celery contains apigenin and other phenolic acids, which, while less potent than the compounds in black garlic or lemon juice, still confer measurable antioxidant benefits (Liu et al., 2020). This finding aligned with prior studies indicating that celery's antioxidant capacity, though moderate, is sufficient to support its inclusion in functional food formulations. The intermediate antioxidant profile of celery underscores its role as a complementary ingredient, balancing nutritional diversity with structural stability in 3D-printed pastes.

Avocado-derived type IV emerged as the most antioxidant-rich formulation (34.84 mg/mL) due to its unique phytochemical composition. Avocados are abundant in lipophilic antioxidants such as carotenoids, tocopherols, and glutathione, which exhibit potent free radical scavenging activity (Chung

et al., 2022). The fruit's high monounsaturated fat content may further enhance the bioavailability of these compounds, amplifying their *in vitro* antioxidant efficacy. This superior performance positions avocado as a key ingredient for developing functional foods to combat oxidative damage, particularly in applications requiring nutrient-dense formulations with robust health benefits (Pal and Raj, 2023).

The systematic quantification of antioxidant levels across formulations elucidates the health implications of ingredient selection in 3D food printing. While all samples demonstrated measurable antioxidant activity, avocado's exceptional performance highlighted its potential as a primary component for oxidative stress alleviation. Similarly, lemon juice (Ali et al., 2020) and fermented black garlic (Tahir et al., 2022) offered complementary benefits, enriching formulations with diverse bioactive compounds. These findings emphasised the importance of tailoring ingredient-hydrocolloid matrices to optimise nutritional and functional outcomes. By integrating ingredients with varied antioxidant mechanisms, 3D-printed foods can be engineered to deliver targeted health benefits, advancing personalised nutrition paradigms within sustainable food systems.

Carbohydrate analysis of pastes

The carbohydrate content of the formulated quantified using **UV-Vis** pastes spectrophotometry, a method validated constructing a glucose standard curve. This approach colorimetric reactions carbohydrates and specific reagents, enabling indirect estimation of carbohydrate concentrations via absorbance measurements. Figure 3b illustrates that the base paste exhibited a baseline carbohydrate concentration of 2.15 g/mL, while the formulated pastes demonstrated some variations. Type I, enriched with black garlic, displayed the highest carbohydrate content at 12.66 g/mL, a result attributed to the inherent fermentable sugars and polysaccharides generated during black garlic's prolonged fermentation process (You et al., 2011; Chua et al., 2022). This substantial increase underscored the dominant influence of black garlic's compositional profile on the paste's carbohydrate load, positioning type I as a high-energy formulation suitable for applications requiring elevated caloric density.

Types II and III pastes exhibited markedly lower carbohydrate concentrations at 3.63 and 3.33 g/mL, respectively. The moderate carbohydrate level in type II, formulated with lemon juice, aligned with the known composition of citrus-derived ingredients, which contain trace amounts of glucose, fructose, and sucrose (Jamil *et al.*, 2015). The slightly low carbohydrate content of type III (3.33 g/mL) reflected the contribution of celery, a vegetable characterised by modest natural sugars and a higher proportion of dietary fibre. These findings highlighted the role of primary ingredients in modulating carbohydrate profiles, with lemon juice and celery imparting distinct nutritional characteristics that may appeal to low-carbohydrate dietary preferences.

Type IV, formulated with avocado, exhibited an intermediate carbohydrate concentration of 8.49 g/mL, surpassing types II and III but remaining lower than type I. Avocado's carbohydrate profile is predominantly composed of dietary fibre and monosaccharides, as documented by Salazar-López et al. (2020), which aligned with the observed values. This balance positioned type IV as a nutritionally versatile option, offering soluble fibre benefits and moderate energy content. The variance carbohydrate levels across formulations underscored the feasibility of tailoring ingredient matrices to achieve specific nutritional targets, a critical consideration for personalised 3D-printed foods. By leveraging the intrinsic properties of fruits and vegetables, these formulations exemplify potential to harmonise structural printability with dietary customisation.

Vitamin C analysis of pastes

Vitamin C (ascorbic acid) was quantified in the formulated pastes via iodine titration, a method grounded in the redox reaction between ascorbic acid and standardised iodine solution (Pehlivan, 2017). This approach relies on the stoichiometric oxidation of ascorbic acid to dehydroascorbic acid, with the endpoint determined by the persistence of a stable iodine-starch complex colour for 20 sec. In the present work, the standardised ascorbic acid solution required 86.43 mL of iodine to reach the endpoint. establishing a reference for subsequent sample analyses. The measured vitamin C concentrations across the samples—base paste (0.003717 g/mL), type I (0.003108 g/mL), type II (0.005775 g/mL), type III (0.003024 g/mL), and type IV (0.002562 g/mL)—revealed disparities (Figure 3c). These variations underscored the influence of ingredient composition on ascorbic acid retention, and highlighted the potential for targeted nutritional customisation in 3D-printed food formulations.

Type II, enriched with lemon juice, exhibited the highest vitamin C concentration (0.005775 g/mL), surpassing the base paste by 55%. This result aligned with the well-documented abundance of ascorbic acid in citrus fruits, where lemon juice is a potent natural source (Jafari et al., 2019). The elevated levels in type II make it a nutritionally advantageous formulation for applications requiring antioxidant enrichment or immune-supportive properties. Conversely, type IV, formulated with avocado, displayed the lowest concentration (0.002562 g/mL), reflecting avocado's inherently lower ascorbic acid content. This stark contrast underscored the critical role of ingredient selection in modulating vitamin C profiles, particularly for dietary solutions tailored to specific micronutrient requirements.

The base paste used as the reference (0.003717 g/mL) was a benchmark for evaluating deviations in content ascorbic acid across experimental formulations. Type Ι (black garlic-enriched) exhibited a marginal reduction (0.003108 g/mL) compared to the base, suggesting minimal contribution of black garlic to vitamin C retention. Type III, containing celery, demonstrated a comparable concentration (0.003024 g/mL) to the base, indicating that celery's moderate ascorbic acid content neither significantly enhanced nor diminished the overall vitamin C profile. These subtle differences emphasised the need for precise formulation control, as even minor compositional shifts can impact nutritional outcomes, particularly in personalised dietary applications where micronutrient precision is paramount.

The nutritional implications of these findings are substantial. Higher vitamin C concentrations, as observed in type II, enhance antioxidant capacity and immune-supportive benefits, aligning with dietary recommendations for combating oxidative stress (Jafari *et al.*, 2019). Conversely, formulations like type IV, with reduced ascorbic acid levels, may necessitate supplementation if targeting populations with elevated vitamin C requirements. These results demonstrated the feasibility of tailoring 3D-printed foods to specific nutritional niches, whether for antioxidant-rich diets or low-acid formulations, by strategically leveraging ingredient-specific vitamin C profiles. Such customisation advanced personalised

nutrition, and aligned with sustainable food innovation, where ingredient-driven nutrient optimisation reduces reliance on synthetic fortification.

Nutritional profile of pastes

The integrated nutritional assessment of the formulated pastes—encompassing antioxidant activity, vitamin C content, and carbohydrate levels—revealed distinct compositional profiles tailored to diverse dietary needs (Figure 3d). As a reference, the base paste exhibited intermediate antioxidant activity alongside a vitamin concentration of 0.003717 g/mL and a carbohydrate content of 2.15 g/mL. This balanced profile positioned the base formulation as a versatile benchmark, suitable for general dietary applications requiring moderate nutrient density. Its antioxidant capacity, though not the highest among the samples, indicated the presence of scavenging compounds capable of mitigating oxidative stress, while its carbohydrate content aligned with foundational energy requirements. This multiparametric analysis underscored the feasibility of leveraging base formulations as platforms for targeted nutritional enhancements.

Antioxidant activity varied markedly across the experimental pastes, reflecting the influence of ingredient-specific bioactive compounds. Sample I, enriched with black garlic, demonstrated superior antioxidant performance compared to the base paste, a finding attributable to the polyphenols and sulphurcontaining compounds inherent to fermented black garlic. Sample IV, formulated with avocado, exhibited antioxidative capacity comparable to the base paste, likely driven by avocado's lipid-soluble antioxidants such as tocopherols and carotenoids. In contrast, samples II and III, incorporating lemon juice and celery, displayed moderate antioxidant activities. These results highlighted the potential of ingredient selection to modulate oxidative stress mitigation, with black garlic and avocado emerging as potent candidates for antioxidant-rich formulations. The observed disparities underscored the importance of compositional synergy in optimising functional properties for health-centric food applications.

Vitamin C and carbohydrate profiles further delineated the nutritional utility of each formulation. With lemon juice as the primary component, sample II achieved the highest vitamin C concentration (0.005775 g/mL), enhancing its suitability for

immune-supportive diets. Conversely, sample IV recorded the lowest vitamin C content (0.002562 g/mL), consistent with avocado's lower ascorbic acid levels. Carbohydrate analysis revealed that sample I (12.66 g/mL) and sample IV (8.49 g/mL) served as high-energy options, with black garlic's fermentable sugars and avocado's dietary fibre contributing distinctively to their carbohydrate matrices. Samples II (3.63 g/mL) and III (3.33 g/mL), characterised by moderate carbohydrate levels, would cater to balanced dietary regimes requiring controlled caloric intake. These findings emphasised ingredient selection's dual role in achieving structural functionality and nutritional precision, which is critical for advancing personalised 3D-printed foods tailored to specific metabolic or health objectives.

The present work examined pre-printing nutritional profiles, noting that the mild processing conditions, including room-temperature extrusion via syringe and minimal thermal exposure, likely facilitated nutrient retention. Type II, characterised by a high lemon juice content, maintained a moderate level of vitamin C (0.005775 g/mL), indicating that cold processing effectively preserved this heatsensitive nutrient. Type IV (avocado-rich) demonstrated the highest antioxidant activity at 34.84 suggesting avocado-derived mg/mL, that antioxidants remained stable under low-shear extrusion conditions. These observations were consistent with research indicating that non-thermal methods reduced nutrient degradation (Bebek Markovinović, 2024). Future research should explicitly compare nutrient levels before and after printing to quantify retention rates. However, our findings indicated that the selected processing parameters, such as ambient temperature and short extrusion time, were advantageous for preserving essential nutrients.

Sample I emerged as a nutritionally robust formulation, combining elevated antioxidant activity, a moderate vitamin C concentration (0.003108 g/mL), and the highest carbohydrate content (12.66 g/mL), positioning it as a multifunctional option for dietary applications requiring enhanced energy density and oxidative stress mitigation. Black garlic's fermentable sugars and bioactive compounds drove this unique profile, synergistically contributing to its high carbohydrate load and antioxidant capacity (You et al., 2011; Chua et al., 2022). In contrast, samples II, III, and IV offered more balanced nutritional

matrices, catering to diverse dietary preferences. Sample II's lemon juice-derived vitamin C (0.005775 g/mL) and moderate carbohydrates (3.63 g/mL) aligned with low-calorie, antioxidant-rich diets (Jamil et al., 2015; Jafari et al., 2019), while sample III's celery-enriched formulation provides a fibre-forward, moderate-carbohydrate alternative. Sample IV, leveraging avocado's dietary fibre and lipid-soluble antioxidants, delivered a mid-range carbohydrate profile (8.49 g/mL) with sustained energy release (Salazar-López et al., 2020). These distinctions underscored the potential for precision nutrition in 3D food printing, where ingredient-specific synergies can be harnessed to meet targeted health outcomes, such as immune support or metabolic management. Future research should focus on isolating key bioactive components, such as black garlic's polyphenols or avocado's tocopherols, to elucidate their mechanistic roles in human health, thereby refining formulations for optimised functional and nutritional efficacy.

Rheological properties of pastes

Based on Figure 4, type I paste exhibits shear-thinning behaviour, as evidenced by the inverse relationship between shear rate and viscosity (e.g., viscosity decreased from ~7.48 to ~0.19 Pa·s as shear rate increased from 1 to 100 1/s). This non-Newtonian characteristic suggested reduced flow resistance under higher stress, typical of pseudoplastic materials. Anomalously, viscosity increased at ~25 1/s (1.15 Pa·s), hinting at potential yield stress or transient structural recovery, though temperature remained stable (~25°C), ruling out thermal effects. Such properties are advantageous for applications requiring controlled flow, like extrusion or coating, where viscosity adapts to applied shear forces.

Similarly, type II paste demonstrated shear-thinning behaviour, decreasing viscosity from ~11.17 to ~0.20 Pa·s as shear rate increased from 1 to 100 1/s, indicating reduced flow resistance under higher shear. Unlike type I, no anomalous viscosity increase suggested a more consistent pseudoplastic response without structural recovery or yield stress effects. The stress gradually increased with shear rate (11.17 Pa to 20.40 Pa), reflecting the balance between increasing deformation and decreasing viscosity. Temperature stability (~25°C) confirmed the absence of thermal degradation or thixotropy. This predictable shear-dependent thinning makes type II suitable for

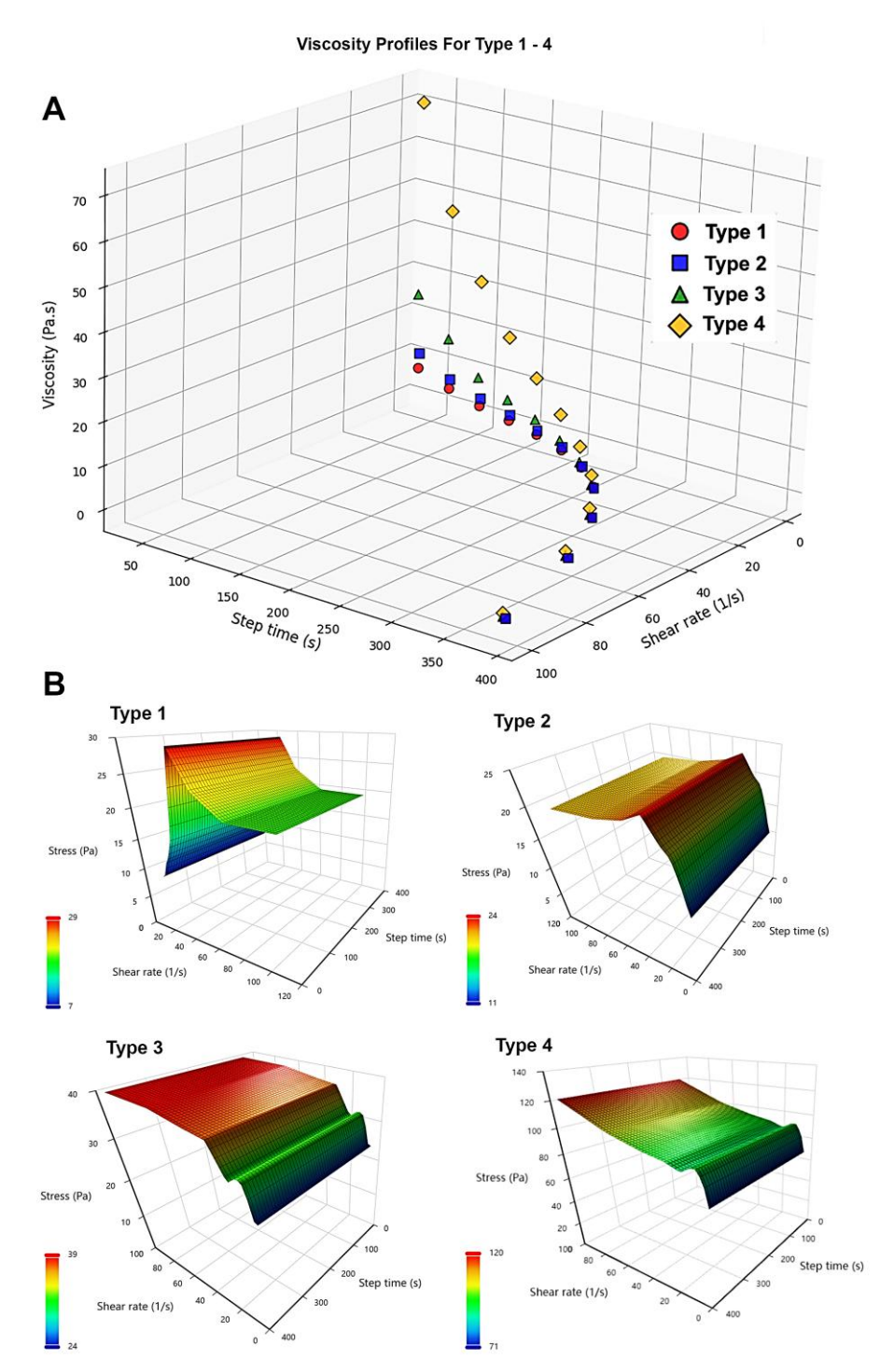


Figure 4. Rheological characterisation of formulated pastes. **(A)** Viscosity (Pa·s) as a function of step time (s) and shear rate. **(B)** Shear stress (Pa) as a function of shear rate (1/s) and step time for types 1 to 4. All formulations exhibit shear-thinning behaviour, a prerequisite for extrusion-based 3D printing, where viscosity decreases under applied shear rates to enable smooth flow through the nozzle while retaining structural integrity post-deposition. Based on the data, type 3 displays the most stable viscosity profile over time, suggesting consistent printability, whereas type 4 demonstrates elevated stress resistance at higher shear rates, indicative of robust mechanical properties under extrusion forces. These profiles highlight the critical role of hydrocolloid-ingredient interactions in tailoring rheological performance for food 3D printing applications. Type 1: 3% (w/w) PS with 1% (w/w) XG; Type 2: 3% (w/w) PS with 2% (w/w) XG; Type 3: 5% (w/w) PS with 2% (w/w) XG; and Type 4: 10% (w/w) PS with 1% (w/w) XG.

processes requiring steady viscosity modulation, such as adhesives or paints, where smooth application under shear is critical.

Type III paste's rheological properties also revealed shear-thinning behaviour, decreasing viscosity from ~25.17 to ~0.39 Pa·s as shear rate increased from 1 to 100 1/s. However, minor viscous irregularities (e.g., a slight increase from 9.72 to 6.94 Pa·s at ~3.98 1/s) suggested transient structural resistance or non-linear flow dynamics, distinct from simpler pseudoplastic fluids. Stress increased with shear rate (25.17 to 39.30 Pa), though a temporary dip at \sim 15.85 1/s (31.08 Pa) hinted at possible yield stress or thixotropic behaviour. The stable temperature (~25°C) confirmed that rheological changes were intrinsic, and not thermally induced.

Type IV paste displayed shear-thinning behaviour, with viscosity decreasing from ~70.65 to ~1.20 Pa·s as shear rate increasing from 1 to 100 1/s, indicating drastic flow resistance reduction under shear. Unlike previous types, stress steadily increased (70.65 to 120.34 Pa) even as viscosity decreased, suggesting energy dissipation or particle alignment effects at high shear rates. Notably, the steepest viscosity drop occurred between 6.3 - 15.8 1/s (~14.84 to ~5.64 Pa·s), highlighting non-linear structural breakdown. The absence of viscosity recovery anomalies and stable temperature (~25°C) ruled out thixotropy or thermal influences.

Conclusion

The present work focused on developing and analysing an avocado-based gel paste suitable for food 3D printing, emphasising optimising structural integrity, nutritional customisation, and printability. The primary goal was to address gaps in existing research by formulating a fruit-based "ink" capable of maintaining shape during extrusion while offering tailored nutritional benefits. Key findings revealed that hydrocolloid composition critically influenced moisture content and texture. For instance, formulations combining PS (5% w/w) and XG (2% w/w) yielded optimal moisture reduction (83.37%), thus enhancing shape retention. Texture analysis identified type 1 paste (3% starch and 1% gum) as superior due to balanced hardness (7.427 N) and minimal adhesiveness (-5.341 N), which are crucial Nutritional for precise printing. assessments highlighted variations in antioxidant activity,

carbohydrates, and vitamin C across samples, with avocado-rich formulations exhibiting the highest antioxidant levels (34.84 mg/mL) and black garlic-enriched pastes exhibiting the highest carbohydrate levels (12.66 g/mL). These results underscored the interplay between ingredient selection, hydrocolloid ratios, and functional properties in 3D food printing.

The present work could advance food technology by demonstrating how ingredienthydrocolloid interactions can be harnessed to create customisable, nutrient-dense printing materials. The successful integration of avocado, black garlic, and other natural components provides a blueprint for developing functional foods tailored to specific dietary needs, such as high-antioxidant or lowcarbohydrate diets. Using cost-effective syringebased testing further offers a practical framework for rapid prototyping, reducing reliance on specialised equipment. These contributions are important for culinary innovation, particularly in personalised nutrition for medical diets or space exploration, where precise nutrient control is critical. The emphasis on minimal thermal processing also suggests potential for preserving heat-sensitive nutrients, aligning with growing consumer demand for healthier, minimally processed foods.

Rheological property of type 3 exhibited a stable viscosity profile over time, ensuring consistent printability, while type 4 demonstrated heightened stress resistance at elevated shear rates (> 50 s⁻¹), thus ideal for high-force extrusion. This divergence stemmed from hydrocolloid interactions: type 3's optimised water-binding capacity promoted stability, whereas type 4's molecular cohesion enhanced mechanical resilience. Such tailored rheological behaviours would enable precise control over structural fidelity and extrusion efficiency in food 3D printing. These insights reflect ingredienthydrocolloid synergy in balancing printability and functional performance for advanced culinary applications.

While the present work concentrated on physicochemical and nutritional properties, it is important to note that sensory evaluations, including taste, texture, and aroma, were not performed, even though they are essential for consumer acceptability. Texture attributes, including hardness adhesiveness (Figure 2), imply mouthfeel compatibility. However, direct sensory testing is necessary to confirm palatability. For example, the

fermented sweetness of black garlic or the acidity of lemon juice may attract particular preferences, while the creaminess of avocado could improve texture perception. Hence, future research should incorporate sensory panels to evaluate acceptability, ensuring that formulations meet consumer expectations. The practical application of these pastes may prioritise nutrient customisation over flavour profiling, focusing on niche markets (e.g., medical diets) where taste is secondary to nutritional requirements. This highlights limitation the necessity interdisciplinary collaboration to reconcile technical feasibility with sensory appeal.

Furthermore, the synergy between hydrocolloids and key ingredients (*e.g.*, avocado's lipids and lemon juice's acidity) underscores the need for formulation-specific optimisation to balance nutritional goals with structural functionality. Future research should also focus on customising the nutrient profile of the paste to develop a more beneficial formulation for consumer health.

Acknowledgement

The authors would like to express their appreciation to the Laboratory Management Office (PPMKCP), the Faculty of Engineering Technology (FTK), and the Faculty of Applied Sciences and Technology (FAST) at Tun Hussein Onn University of Malaysia (UTHM) for their support. The publication of this work was funded by the UTHM TIER 1 Grant (Vot Q996). The authors would also like to extend their gratitude to all of the food laboratory assistants, for their dedicated assistance throughout this project.

References

- Alfadul, S. M. and Hassan, B. H. 2016. Chemical composition of natural juices combining lemon and dates. International Journal of Food Engineering 2(1): 9-15.
- Ali, S. H., Obaid, Q. A. and Awaid, K. G. 2020. Lemon juice antioxidant activity against oxidative stress. Baghdad Science Journal 17(1): 31.
- Bebek Markovinović, A. 2024. Application of hurdle technology and 3D printing in the development of strawberry based functional food. Croatia: University of Zagreb, PhD thesis.

- Bedrníček, J., Laknerová, I., Lorenc, F., Moraes, P. P., Jarošová, M., Samková, E., ... and Smetana, P. 2021. The use of a thermal process to produce black garlic: Differences in the physicochemical and sensory characteristics using seven varieties of fresh garlic. Foods 10(11): 2703.
- Bhat, Z. F., Morton, J. D., Kumar, S., Bhat, H. F., Aadil, R. M. and Bekhit, A. E.-D. A. 2021. 3D printing: Development of animal products and special foods. Trends in Food Science and Technology 118: 87-105.
- Božinović, M., Sokač, T., Šalić, A., Dukarić, A.-M., Tišma, M., Planinić, M. and Zelić, B. 2023. Standardization of 3, 5-dinitrosalicylic acid (DNS) assay for measuring xylanase activity: Detecting and solving problems. Croatian Journal of Food Science and Technology 15(2): 151-162.
- Choudhary, S., Noor, M. U., Hussain, M. S., Mishra, M. and Tyagi, S. 2022. Pharmacological properties and phytoconstituents of garlic (*Allium sativum* L.): A review. Biological Sciences 2(4): 338-346.
- Chua, L. S., Abdullah, F. I. and Lim, S. H. 2022. Physiochemical changes and nutritional content of black garlic during fermentation. Applied Food Research 2(2): 100216.
- Chung, S. W., Rho, H., Lim, C. K., Jeon, M. K., Kim, S., Jang, Y. J. and An, H. J. 2022. Photosynthetic response and antioxidative activity of 'Hass' avocado cultivar treated with short-term low temperature. Scientific Reports 12(1): 11593.
- Derossi, A., Caporizzi, R., Oral, M. and Severini, C. 2020. Analyzing the effects of 3D printing process *per se* on the microstructure and mechanical properties of cereal food products. Innovative Food Science and Emerging Technologies 66: 102531.
- Flieger, J. and Flieger, M. 2020. The [DPPH•/DPPH-H]-HPLC-DAD method on tracking the antioxidant activity of pure antioxidants and goutweed (*Aegopodium podagraria* L.) hydroalcoholic extracts. Molecules 25(24): 6005.
- Gu, Y., Schwarz, B., Forget, A., Barbero, A., Martin, I. and Shastri, V. P. 2020. Advanced bioink for 3D bioprinting of complex free-standing structures with high stiffness. Bioengineering

- 7(4): 141.
- Helmenstine, A. M. 2007. Vitamin C determination by iodine titration. Retrieved from ThoughtCo. website: https://www.thoughtco.com/vitamin-c-determination-by-iodine-titration-606322
- Hussain, S., Malakar, S. and Arora, V. K. 2022. Extrusion-based 3D food printing: Technological approaches, material characteristics, printing stability, and post-processing. Food Engineering Reviews 14(1): 100-119.
- Jafari, D., Esmaeilzadeh, A., Mohammadi-Kordkhayli, M. and Rezaei, N. 2019. Vitamin C and the immune system. In Mahmoudi, M. and Rezaei, N. (eds). Nutrition and Immunity, p. 81-102. United States: Springer.
- Jamil, N., Jabeen, R., Khan, M., Riaz, M., Naeem, T., Khan, A., ... and Bazai, Z. A. 2015. Quantitative assessment of juice content, citric acid and sugar content in oranges, sweet lime, lemon and grapes available in fresh fruit market of Quetta city. International Journal of Basic and Applied Sciences 15(1): 21-24.
- Ji, S., Xu, T., Li, Y., Li, H., Zhong, Y. and Lu, B. 2022. Effect of starch molecular structure on precision and texture properties of 3D printed products. Food Hydrocolloids 125: 107387.
- Liu, D.-K., Xu, C.-C., Zhang, L., Ma, H., Chen, X.-J., Sui, Y.-C. and Zhang, H.-Z. 2020. Evaluation of bioactive components and antioxidant capacity of four celery (*Apium graveolens* L.) leaves and petioles. International Journal of Food Properties 23(1): 1097-1109.
- Pal, D. and Raj, K. 2023. Role of lipid-soluble bioactive substance from avocado for inhibition of prostate and other cancers. In Singh, M. (ed). Therapeutic Platform of Bioactive Lipids Focus on Cancer, p. 215-230. United States: Apple Academic Press.
- Pant, A., Lee, A., Karyappa, R., Lee, C. P., An, J., Hashimoto, M., ... and Zhang, Y. 2020. 3D food printing of fresh vegetables using food hydrocolloids for dysphagic patients. Food Hydrocolloids 114: 106546.
- Pehlivan, F. E. 2017. Vitamin C: An antioxidant agent. Vitamin C 2: 23-35.
- Periard, D., Schaal, N., Schaal, M., Malone, E. and Lipson, H. 2007. Printing food. In 2007 International Solid Freeform Fabrication

- Symposium, p. 567-574. United States: The University of Texas at Austin.
- Pulatsu, E. and Lin, M. 2021. A review on customizing edible food materials into 3D printable inks: Approaches and strategies. Trends in Food Science and Technology 107: 68-77.
- Qiu, Z., Zheng, Z., Zhang, B., Sun-Waterhouse, D. and Qiao, X. 2020. Formation, nutritional value, and enhancement of characteristic components in black garlic: A review for maximizing the goodness to humans. Comprehensive Reviews in Food Science and Food Safety 19(2): 801-834.
- Razavi, S. M. and Karazhiyan, H. 2012. Rheological and textural characteristics of date paste. International Journal of Food Properties 15(2): 281-291
- Salazar-López, N. J., Domínguez-Avila, J. A., Yahia, E. M., Belmonte-Herrera, B. H., Wall-Medrano, A., Montalvo-González, E. and González-Aguilar, G. 2020. Avocado fruit and by-products as potential sources of bioactive compounds. Food Research International 138: 109774.
- SavorEat. 2023. 3D food printing: All you need to know. Retrieved from SavorEat website: https://savoreat.com/the-world-of-3d-food-printing/
- Tahir, Z., Saeed, F., Nosheen, F., Ahmed, A. and Anjum, F. M. 2022. Comparative study of nutritional properties and antioxidant activity of raw and fermented (black) garlic. International Journal of Food Properties 25(1): 116-127.
- Tomašević, I., Putnik, P., Valjak, F., Pavlić, B., Šojić, B., Markovinović, A. B. and Kovačević, D. B. 2021. 3D printing as novel tool for fruit-based functional food production. Current Opinion in Food Science 41: 138-145.
- Varvara, R.-A., Szabo, K. and Vodnar, D. C. 2021. 3D food printing: Principles of obtaining digitally-designed nourishment. Nutrients 13(10): 3617.
- Vlaicu, P. A., Untea, A. E., Varzaru, I., Saracila, M. and Oancea, A. G. 2023. Designing nutrition for health—Incorporating dietary by-products into poultry feeds to create functional foods with insights into health benefits, risks, bioactive compounds, food component

- functionality and safety regulations. Foods 12(21): 4001.
- Wang, J., Jiang, Q., Huang, Z., Muhammad, A. H., Gharsallaoui, A., Cai, M., ... and Sun, P. 2024. Rheological and mechanical behavior of soy protein-polysaccharide composite paste for extrusion-based 3D food printing: Effects of type and concentration of polysaccharides. Food Hydrocolloids 153: 109942.
- Xiao, F., Xu, T., Lu, B. and Liu, R. 2020. Guidelines for antioxidant assays for food components. Food Frontiers 1(1): 60-69.
- You, B.-R., Kim, H.-R., Kim, M.-J. and Kim, M.-R. 2011. Comparison of the quality characteristics and antioxidant activities of the commercial black garlic and lab-prepared fermented and aged black garlic. Journal of The Korean Society of Food Science and Nutrition 40(3): 366-371.
- Zhao, Y., Li, Y., Liu, Q., Chen, Q., Sun, F. and Kong, B. 2024. Investigating the rheological properties and 3D printability of tomato-starch paste with different levels of xanthan gum. International Journal of Biological Macromolecules 257: 128430.
- Zhu, S., Stieger, M. A., van der Goot, A. J. and Schutyser, M. A. 2019. Extrusion-based 3D printing of food pastes: Correlating rheological properties with printing behaviour. Innovative Food Science and Emerging Technologies 58: 102214.